Received November 22, 2017, accepted December 28, 2017, date of publication January 4, 2018,
date of current version February 28, 2018.

Digital Object Identifier 10.1109/ACCESS.2018.2789581

Outage Performance Analysis for Wireless Non-Orthogonal Multiple Access Systems

JINGLUN WANG[1], BIN XIA[1], (Senior Member, IEEE), KEXIN XIAO[1], YICHEN GAO[1], AND SHAODAN MA[2]
[1]Shanghai Institute of Advanced Communication and Data Science, Institute of Wireless Communication Technologies, Department of Electronic Engineering, Shanghai Jiao Tong University, Shanghai 200240, China
[2]Department of Electrical and Computer Engineering, University of Macau, Macao 999078, China

Corresponding author: Bin Xia (bxia@sjtu.edu.cn)

This work was supported in part by the National Key Research and Development Program of China under Grant 2016YFE0121100, in part by the Huawei HIRP Project under Grant YB2015040062, in part by the Key Laboratory of Wireless Sensor Network and Communication, Chinese Academy of Sciences under Grant 2015002, in part by the National Nature Science Foundation of China under Grant 61771307, Grant 61601524, Grant 61521062, and Grant 61401274, and in part by the Macau Science and Technology Development Fund under Grant 091/2015/A3 and Grant 020/2015/AMJ.

ABSTRACT Non-orthogonal multiple access (NOMA) is a promising air-interface technology for its ability to support massive wireless mobile terminals. In this paper, the outage performance for uplink NOMA systems employing the dynamic ordered successive interference cancellation receiver is analyzed under the independent but not identically distributed (i.ni.d.) fading environment. We theoretically reveal the general approach to derive the closed-form outage probability expression for an arbitrary number of serving users. Under the i.ni.d. fading environment, the probability for each possible decoding order is derived respectively based on the observation of the time-varying received power strength for each user. Furthermore, encountering the challenge of solving the multidimensional integration, a recursive method is proposed to deal with the conditional outage probabilities under a certain decoding order as a joint probability problem with the linear constraints of the decoding order and the required data rate. Finally, we derive the closed-form outage probability expressions. The simulations are performed to validate the accuracy of the theoretical results and reveal the superiority of the dynamic mode over the fixed one.

INDEX TERMS Uplink NOMA, dynamic ordered SIC decoding, outage probability, interference-limited system.

I. INTRODUCTION

To support a large number of connected devices in high data rate and high spectral efficiency wireless communications, Non-orthogonal multiple access (NOMA) has been highly recommended as a promising access technology for the fifth generation (5G) wireless communication networks [1]. The code superposition takes the advantage of the power domain to transmit the multi-user signals [2]. On the receiver side, the successive interference cancellation (SIC) is applied for multi-user detection [3] and [4]. NOMA is proved feasible to achieve higher spectrum efficiency and to accommodate more mobile terminals simultaneously for overloaded communication networks [5].

Many research activities have been initiated to analyze the performance of the downlink NOMA system. Tabassum *et al.* [6] and Ding *et al.* [7] analyze the outage performance for a system with randomly located users by leveraging the order statistic method, where the channels are modeled as independent identical distribution (i.i.d.) variables. Moreover, Yue *et al.* [8] study the performance of NOMA systems with applying the cooperative techniques over Nakagami-*m* fading channels. Actually, in order to tackle the outage probability in downlink NOMA systems, a simplified assumption has always been adopted, i.e., the i.i.d. fading channels. Thanks to the order statistics, instead of traversing all possible decoding orders, the general outage performance could be effectively derived. However, with respect to the uplink NOMA system, it is more practical to consider the independent nonidentical distributed (i.ni.d.) Rayleigh fading environment, due to the fact that signals from different users suffer from uncorrelated channel fading with different transmit power and different path loss. Thus, several research has been studied for uplink NOMA systems under i.ni.d. fading environment. In [9], the closed-form outage probability expressions are derived for a two-user scenario with the fixed decoding order. In [10], the dynamic user clustering and power allocation for uplink and downlink NOMA systems are investigated to maximize the sum-throughput in a cell. Moreover, a dynamic power allocation scheme in [11] and a dynamic decoding order strategy in [12] are proposed for a two-user or three-user uplink NOMA system, respectively. However, there are some limitations to performance analysis due to the assumption of the fixed number of users. The general expressions of the outage performance have not been revealed when the user number increases in uplink NOMA systems.

With more devices connected, it is a high challenge to derive the closed-form expressions of the outage probability in the uplink NOMA system. Under the i.ni.d. Rayleigh fading environment, outage events with different decoding order are obviously disparate from each other and no similar cases can be simply merged by the order statistic method. Moreover, increasing the number of the users, it is difficult to apply a general approach for the closed-form expressions of the specific user's conditional outage probability which is formulated as a complicated joint probability problem with the linear constraints of the decoding order and the target data rate. Therefore the outage analysis issue is indeed important and challengeable.

To solve the above problems, for the uplink NOMA system, we theoretically analyze the outage performance for both of the dynamic and fixed ordered SIC receivers with an arbitrary number of users. Our contribution is summarized as follows:

- We compare two advanced multiuser detection schemes in the interference-limited uplink NOMA system, the dynamic-ordered SIC receiver and the fixed-ordered one. Instead of the assumption of i.i.d. fading channels, we theoretically analyze the outage performance in i.ni.d. fading environment for the arbitrary number of users.
- We derive the closed-form outage probability expressions for the dynamic decoding mechanism. We expose a general method to analyze the outage performance when an arbitrary number of users are served simultaneously. Firstly, the probability for each possible decoding order is derived. Moreover, a recursive method is proposed to deal with the complicated multidimensional integral problem with the arbitrary number of users.
- We derive the closed-form outage probability expressions of any specific user with the fixed ordered decoding receiver for comparison. Finally, theoretical evaluations and numerical simulations are conducted. The results verify the accuracy of the theoretical analysis and reveal the superiority of the dynamic mode over the fixed one.

The rest of the paper is organized as follows. Section II describes the system model and two advanced SIC receivers. In Section III, the outage probabilities performance is analyzed for the uplink NOMA system. Section IV presents the simulation results, followed by Section V that concludes this paper.

II. SYSTEM MODEL

We consider a single-cell uplink wireless network with a central-located base station (BS) and M users. It is assumed that all the users and the BS are equipped with single antenna. All users are served by sharing the same wireless channel. The channel coefficient between the user m and the BS is denoted by $h_m = \frac{g_m}{PL(d_m)}$, where large-scale fading component $PL(d_m)$ denotes the path loss for the user m located d_m away from the BS and g_m represents the small scale Rayleigh fading channel gain, subjecting to complex Gaussian distribution with zero mean and unit variance. To simplify the analysis, $PL(d_m)$ is modelled by Free-Space path loss model [9], i.e., $PL(d_m) = (\frac{\sqrt{G_l} l}{4\pi d_m})$, where G_l is the product of the transmit and receive antenna field radiation patterns in the line-of sight (LOS) direction, and l is the signal weavelength. Since all the users are scheduled simultaneously on the same recourse, the received signal at the BS can be written as

$$Y = \sum_{m=1}^{M} h_m \sqrt{p_m} s_m + n, \tag{1}$$

where s_m is the transmitted message of the user m with $\mathbb{E}\{|s_m|^2\} = 1$, p_m is the transmit power for the user m and n denotes the zero-mean additive white Gaussian noise with the variance σ^2. For the sake of simplicity, we use $w_m \triangleq p_m|h_m|^2$ and $\lambda_m \triangleq \frac{1}{\mathbb{E}(w_m)}$ to denote the instantaneous received signal power and its mean value, respectively. Then, the random variable w_m is exponentially distributed with parameter λ_m. The probability density function (PDF) of w_m can be formulated as

$$f_{w_m}(x) = \lambda_m e^{-\lambda_m x}. \tag{2}$$

Next, we consider two different SIC decoding schemes according to the short term and long term received power of each user, respectively. It is assumed that the SIC receiver can perfectly extract each user's signal power from the received signal when the decoding is successful.

A. DYNAMIC-ORDERED SIC RECEIVER

For the dynamic ordered scheme, the channel state information (CSI) is perfectly known at the BS [13]. Before decoding, the receiver determines the decoding order based on the instantaneous received signal power of each user. The instant decoding order can be represented by a permutation π. Following the decoding order π, the users are decoded in the sequence of $[\pi_1, \pi_2, \cdots, \pi_M]$ with the instantaneous received signal power relation: $w_{\pi_1} > \cdots > w_{\pi_M}$. When decoding the message of the user π_m, the SIC receiver should decode all the prior $(m-1)$ users' message first, then reconstruct and subtract regenerated multiuser interference from the superimposed signal. Meanwhile, the rest $(M-m)$ users' signals are regarded as the inter-user interference.

B. FIXED-ORDERED SIC RECEIVER

For the fixed ordered scheme, it is assumed that the BS determines the decoding order only by considering the statistic

CSI for each user, i.e. the average received power of each user. Therefore, according to the large-scale fading channel model employed in this paper, the users are decoded in the sequence of $1, 2, \cdots, M$ based on their distance to the BS, i.e., $d_1 < d_2 < \cdots < d_M$.

III. OUTAGE PERFORMANCE ANALYSIS FOR TWO TYPE OF SIC RECEIVERS

In this section, we theoretically analyze the outage performance for a M-users uplink NOMA system with the dynamic-ordered and fixed-ordered SIC receivers. Noise can be safely neglected in a dense interference-limited wireless system [14], where the inevitable inter-user interference is dominant.

A. THEORETICAL ANALYSIS FOR DYNAMIC ORDERED SIC RECEIVER

By applying the dynamic ordered decoding scheme, the instant decoding order π is determined by the instantaneous received signal power of each user. Thus, the achievable data rate of the user π_m where $m \neq M$ under a given decoding order π can be formulated as

$$R_{\pi_m} = \log\left(1 + \frac{w_{\pi_m}}{\sum_{i=m+1}^{M} w_{\pi_i}}\right). \tag{3}$$

And the achievable data rate for the last decoded user π_M can be presented as following, where the multiuser interference has been ideally detected and eliminated,

$$R_{\pi_M} = \log\left(1 + \frac{w_{\pi_M}}{\sigma^2}\right). \tag{4}$$

where σ^2 is the variance of the white Gaussian noise.

In such a case, if the channel condition becomes worse and cannot guarantee the reliability of the transmission, i.e., the achievable rate is less the target rate, the outage may occur [15], [16]. Hence, we first define the event $E^c_{m|\pi}$ that the achievable data rate R_{π_m} of the user π_m is larger than the target data rate $\hat{R}_{\pi_m}$ under a given decoding order π. Therefore, the probability of $E^c_{m|\pi}$ can be formulated as

$$\mathbb{P}(E^c_{m|\pi}) = \mathbb{P}(R_{\pi_m} \geq \hat{R}_{\pi_m} \mid \pi). \tag{5}$$

After obtaining $\mathbb{P}(E^c_{m|\pi})$, the outage probability of the user π_m under a given decoding order π is expressed as

$$\mathbb{P}^{out}_{m|\pi} = 1 - \prod_{l=1}^{m} \mathbb{P}\big(E^c_{l|\pi}\big). \tag{6}$$

For a specific user, its decoding order changes with the instantaneous received power at the BS. Therefore, the outage probability of the user m is derived by

$$\mathbb{P}^{out}_{m} = \mathbb{E}_{\Pi}\{\mathbb{P}^{out}_{m|\pi}\} = \sum_{\pi\in\Pi, m=\pi_m} \mathbb{P}(\pi) \times \mathbb{P}^{out}_{m|\pi} \tag{7}$$

where Π is the set of all possible decoding orders and $\mathbb{E}_{\Pi}$ is the expectation with respect to all π in Π.

Obviously, $\mathbb{P}(E^c_{m|\pi})$ can be written as (8), where $\mathbb{P}(x, y)$ represents the joint probability that events x and y occur concurrently,

$$\mathbb{P}(E^c_{m|\pi}) = \frac{\mathbb{P}(R_{\pi_m} \geq \hat{R}_{\pi_m}, \pi)}{\mathbb{P}(\pi)}. \tag{8}$$

To derive the closed-form expression of (8), we first present the following lemma to obtain the denominator $\mathbb{P}(\pi)$.

Lemma 1: The probability of the decoding order π in the set of all possible decoding order Π is given by

$$\mathbb{P}(\pi) = \frac{\prod_{i=2}^{M} \lambda_{\pi_i}}{\prod_{i=2}^{M}\left(\sum_{k=1}^{i} \lambda_{\pi_k}\right)}. \tag{9}$$

Proof: Based on the dynamic-ordered SIC scheme, the instantaneous received signal powers are sorted in the sequence of $w_{\pi_1} > \cdots > w_{\pi_M}$. Accordingly, the decoding order probability can be given by

$$\mathbb{P}(\pi) = \int_0^\infty \lambda_{\pi_M} e^{-\lambda_{\pi_M} w_{\pi_M}} \mathrm{d}w_{\pi_M} \cdots \int_{w_{\pi_3}}^\infty \lambda_{\pi_2} e^{-\lambda_{\pi_2} w_{\pi_2}} \mathrm{d}w_{\pi_2}$$
$$\times \int_{w_{\pi_2}}^\infty \lambda_{\pi_1} e^{-\lambda_{\pi_1} w_{\pi_1}} \mathrm{d}w_{\pi_1} = \frac{\prod_{i=2}^{M} \lambda_{\pi_i}}{\prod_{i=2}^{M}\left(\sum_{k=1}^{i} \lambda_{\pi_k}\right)}. \tag{10}$$

■

For convenience, let $\overline{w}^M_{m+1} = \sum_{i=m+1}^{M} w_{\pi_i}$. When $m \neq M$, the numerator in (8) is given by

$$\mathbb{P}\big(R_{\pi_m} \geq \hat{R}_{\pi_m}, \pi\big) = \mathbb{P}\big(w_{\pi_m} \geq \beta_m \overline{w}^M_{m+1}, \pi\big), \tag{11}$$

where $\beta_m = 2^{\hat{R}_{\pi_m}} - 1$. It should be noted that the joint probability in (11) is highly determined by β_m. Therefore in the following contents, we will discuss the derivation process of (11) for different cases of β_m.

When $\beta_m \geq 1$, $\mathbb{P}(R_{\pi_m} \geq \hat{R}_{\pi_m}, \pi)$ can be derived by the following lemma.

Lemma 2: When $\beta_m \geq 1$, the result of the joint probability $\mathbb{P}(w_{\pi_m} > \beta_m \overline{w}^M_{m+1}, \pi)$ is given by

$$\mathbb{P}(w_{\pi_m} > \beta_m \overline{w}^M_{m+1}, \pi)$$
$$= \frac{\prod_{i=2}^{M} \lambda_{\pi_i}}{\prod_{i=2}^{m}\left(\sum_{k=1}^{i} \lambda_{\pi_k}\right) \prod_{i=m+1}^{M}\left(\sum_{k=m+1}^{i} \lambda_{\pi_k} + (i-m)\beta_m \sum_{j=1}^{m} \lambda_{\pi_j}\right)}. \tag{12}$$

Proof: When $\beta_m \geq 1$, $\beta_m \overline{w}^M_{m+1} > w_{\pi_{m+1}}$ always holds. With this constraint and the given decoding order $w_{\pi_1} > \cdots > w_{\pi_M}$, the joint probability can be easily derived by integration,

$$\mathbb{P}(w_{\pi_m} > \beta_m \overline{w}^M_{m+1}, \pi) \int_0^\infty \lambda_{\pi_M} e^{-\lambda_{\pi_M} w_{\pi_M}} \mathrm{d}w_{\pi_M}$$
$$\cdots \int_{w_{\pi_{m+2}}}^\infty \lambda_{\pi_{m+1}} e^{-\lambda_{\pi_{m+1}} w_{\pi_{m+1}}} \mathrm{d}w_{\pi_{m+1}}$$

$$\times \int_{\beta_m \overline{w}_{m+1}^M}^{\infty} \lambda_{\pi_m} e^{-\lambda_{\pi_m} w_{\pi_m}} \mathrm{d}w_{\pi_m} \cdots \int_{w_{\pi_2}}^{\infty} \lambda_{\pi_1} e^{-\lambda_{\pi_1} w_{\pi_1}} \mathrm{d}w_{\pi_1}. \tag{13}$$

■

When $\beta_m < 1$, the joint probability $\mathbb{P}(w_{\pi_m} > \beta_m \overline{w}_{m+1}^M, \pi)$ equals to the sum of a series probabilities based on the total probability theorem. Then we have

$$\begin{aligned}\mathbb{P}(w_{\pi_m} > \beta_m \overline{w}_{m+1}^M, \pi) &= \sum_{j=0}^{M-m-1} \mathbb{P}\big(w_{\pi_1} > \cdots > w_{\pi_{m+j}} > \beta_m \overline{w}_{m+1}^M \\ &\qquad > w_{\pi_{m+j+1}} \cdots > w_{\pi_M}\big) \\ &\quad + \mathbb{P}\big(w_{\pi_1} > \cdots > w_{\pi_M} > \beta_m \overline{w}_{m+1}^M\big).\end{aligned} \tag{14}$$

Furthermore, we reduce the right hand side of (14) to the sum of $K+1$ non-zero probabilities given by (15), shown at the bottom of this page, where $K = \lceil \frac{1}{\beta_m} \rceil - 1$, and $\lceil x \rceil$ means the smallest integer greater than or equal to x. When $K \le M - m - 1$, we have the following lemma.

Lemma 3: If $K = \lceil \frac{1}{\beta_m} \rceil - 1$, the probability $\mathbb{P}_{K+i} = \mathbb{P}(w_{\pi_1} > \cdots > w_{\pi_{m+K+i}} > \beta_m \overline{w}_{m+1}^M > w_{\pi_{m+K+i+1}} \cdots > w_{\pi_M})$ is equal to 0 for $i = 1, \cdots, M-K-m$.

Proof: For $\mathbb{P}_{K+1} = \mathbb{P}(w_{\pi_1} > \cdots > w_{\pi_{m+K+1}} > \beta_m \overline{w}_{m+1}^M > w_{\pi_{m+K+1+1}} \cdots > w_{\pi_M})$, due to the inequality $w_{\pi_{m+K+1}} > \beta_m \overline{w}_{m+1}^M$, we can get

$$w_{\pi_{m+1}} < \frac{1-\beta_m}{\beta_m} w_{\pi_{m+K+1}} - \sum\nolimits_{\substack{i=m+2\\ i\neq m+K+1}}^{M} w_{\pi_i}. \tag{16}$$

Meanwhile, the condition of the decoding order π means $w_{\pi_{m+1}} > w_{\pi_{m+2}}$. Thus, we can have

$$w_{\pi_{m+2}} < \frac{1}{2}\left(\frac{1-\beta_m}{\beta_m} w_{\pi_{m+K+1}} - \sum\nolimits_{\substack{i=m+3\\ i\neq m+K+1}}^{M} w_{\pi_i}\right). \tag{17}$$

By the recursive method, the restrictions of $w_{\pi_{m+K+1}}$ will be derived by

$$\frac{1-(K+1)\beta_m}{\beta_m} w_{\pi_{m+K+1}} > \overline{w}_{m+K+2}^M. \tag{18}$$

According to $K = \lceil \frac{1}{\beta_m} \rceil - 1$, we can get $\frac{1}{K+1} \le \beta_m < \frac{1}{K}$, which means $1-(K+1)\beta_m \le 0$. As a result, $\mathbb{P}_{K+1}$ equals to 0. Then, it can be concluded that $\mathbb{P}_{K+i} = 0$ for $i = 1, \cdots, M-K-m$ by the same token. Hitherto, the proof is completed. ■

Because the value of $\beta_m \overline{w}_{m+1}^M$ is constrained by the decoding order and the target data rate, the joint probability $\mathbb{P}(w_{\pi_m} > \beta_m \overline{w}_{m+1}^M, \pi)$ is divided into three disjoint cases of Q_1, Q_2 and Q_3 based on the total probability theorem. We can directly get the result of Q_1 by integration in (19), shown at the bottom of this page, Furthermore, to obtain Q_3, for $1 \le j \le K-1$, we specify the integral domain of $w_{\pi_{m+j}}$ as following:

$$w_{\pi_{m+j+1}} < w_{\pi_{m+j}} < \frac{1}{j}\left(\frac{1-\beta_m}{\beta_m} w_{\pi_{m+K}} - \sum_{\substack{i=m+j+1\\ i\neq m+K}}^{M} w_{\pi_i}\right). \tag{20}$$

And $w_{\pi_{m+K}}$ satisfies $w_{\pi_{m+K}} > \frac{\beta_m}{1-K\beta_m} \overline{w}_{m+K+1}^M$, because of $\frac{1}{K+1} \le \beta_m < \frac{1}{K}$, $\frac{\beta_m}{1-K\beta_m} \ge 1$ and $\frac{\beta_m}{1-K\beta_m} \overline{w}_{m+K+1}^M > w_{\pi_{m+K+1}}$. Consequently, the result of Q_3 can be

$$\begin{aligned}\mathbb{P}(w_{\pi_m} > \beta_m \overline{w}_{m+1}^M, \pi) &= \underbrace{\mathbb{P}(w_{\pi_1} > \cdots > w_{\pi_m} > \beta_m \overline{w}_{m+1}^M > w_{\pi_{m+1}} > \cdots > w_{\pi_M})}_{Q_1} \\ &\quad + \underbrace{\sum\nolimits_{j=1}^{K-1} \mathbb{P}(w_{\pi_1} > \cdots > w_{\pi_{m+j}} > \beta_m \overline{w}_{m+1}^M > w_{\pi_{m+j+1}} \cdots > w_{\pi_M})}_{Q_2} \\ &\quad + \underbrace{\mathbb{P}(w_{\pi_1} > \cdots > w_{\pi_{m+K}} > \beta_m \overline{w}_{m+1}^M > w_{\pi_{m+K+1}} \cdots > w_{\pi_M})}_{Q_3}\end{aligned} \tag{15}$$

$$\begin{aligned}Q_1 &= \int_0^{\infty} \lambda_{\pi_M} e^{-\lambda_{\pi_M} w_{\pi_M}} \mathrm{d}w_{\pi_M} \cdots \int_{w_{\pi_{m+2}}}^{\frac{\beta_m}{1-\beta_m}\overline{w}_{m+2}^M} \lambda_{\pi_{m+1}} e^{-\lambda_{\pi_{m+1}} w_{\pi_{m+1}}} \mathrm{d}w_{\pi_{m+1}} \int_{\beta_m \overline{w}_{m+1}^M}^{\infty} \lambda_{\pi_m} e^{-\lambda_{\pi_m} w_{\pi_m}} \mathrm{d}w_{\pi_m} \cdots \int_{w_{\pi_2}}^{\infty} \lambda_{\pi_1} e^{-\lambda_{\pi_1} w_{\pi_1}} \mathrm{d}w_{\pi_1} \\ &= \frac{\prod\limits_{i=2}^{M} \lambda_{\pi_i}}{\prod\limits_{i=2}^{m} (\sum\limits_{j=1}^{i} \lambda_{\pi_j})} \left[\frac{1}{\prod\limits_{i=m+1}^{M} \left(\sum\limits_{j=m+1}^{M} \lambda_{\pi_j} + (i-m)\beta_m \sum\limits_{j=1}^{m} \lambda_{\pi_j} \right)} \right. \\ &\qquad \left. - \frac{1}{(\lambda_{\pi_{m+1}} + \beta_m \sum\limits_{i=1}^{m} \lambda_{\pi_i}) \prod\limits_{i=m+2}^{M} \left(\sum\limits_{j=m+2}^{i} \lambda_{\pi_j} + (i-m-1)\frac{\beta_m}{1-\beta_m} \sum\limits_{i=1}^{m+1} \lambda_{\pi_i} \right)} \right]\end{aligned} \tag{19}$$

derived by

$$Q_3 = \int_0^\infty \lambda_{\pi_M} e^{-\lambda_{\pi_M} w_{\pi_M}} \mathrm{d}w_{\pi_M} \cdots \int_{\frac{\beta_m}{1-K\beta_m}\overline{w}_{i+K+1}^M}^\infty \lambda_{\pi_{m+K}} e^{-\lambda_{\pi_{m+K}} w_{\pi_{m+K}}} \mathrm{d}w_{\pi_{m+K}} \cdots \int_{w_{\pi_{m+j+1}}}^{\frac{1}{j}\left(\frac{1-\beta_m}{\beta_m} w_{\pi_{m+K}} - \sum_{i=m+j+1, i\neq m+K}^{M} w_{\pi_i}\right)} \lambda_{\pi_{m+j}} e^{-\lambda_{\pi_{m+j}} w_{\pi_{m+j}}} \mathrm{d}w_{\pi_{m+j}} \cdots \int_{w_{\pi_{m+1}}}^\infty \lambda_{\pi_m} e^{-\lambda_{\pi_m} w_{\pi_m}} \mathrm{d}w_{\pi_m} \cdots \int_{w_{\pi_2}}^\infty \lambda_{\pi_1} e^{\lambda_{\pi_1} w_{\pi_1}} \mathrm{d}w_{\pi_1}. \quad (21)$$

The closed-form expression of (21) is accessible when the numerical values of β_m, m and M are provided. It is because of that the unidimensional integral domain for any variable w_{π_i} is the function of the variables with the index higher than i and the probability density function (pdf) of each variable is the basic exponential function.

Based on Lemma 4, each probability of Q_2 can be obtained by recursive calculation. And for $\mathbb{P}(w_{\pi_m} > \beta_m \overline{w}_{m+1}^M, \pi)$ with $\frac{1}{K+1} \leq \beta_m < \frac{1}{K}$, there are $2^{K+1} - 1$ different values of probabilities to be calculated which is similar as the method in (19) and (21).

Lemma 4: To obtain the closed-form expression of the $(j-1)$-th probability in Q_2, there are $2^{K-j} - 1$ independent joint probabilities to be calculated by basic exponential integration. And each disjoint integration domain can be obtained by the recursive method.

Proof: For the last probability $J_{K-1} = \mathbb{P}(w_{\pi_1} > \cdots w_{\pi_{m+K-1}} > \beta_m \overline{w}_{m+1}^M > w_{\pi_{m+K}} \cdots w_{\pi_M})$ in Q_2, we can divide this joint probability into two disjoint cases of $\mathbb{P}^1_{J_{K-1}}$ and $\mathbb{P}^2_{J_{K-1}}$ based on the total probability theorem as following,

$$J_{K-1} = \mathbb{P}^1_{J_{K-1}} + \mathbb{P}^2_{J_{K-1}}. \quad (22)$$

The integration domains of $\mathbb{P}^1_{J_{K-1}}$ and $\mathbb{P}^2_{J_{K-1}}$ are $\Omega_{P^1_{J_{K-1}}}$ and $\Omega_{P^2_{J_{K-1}}}$, which can be written as (23) and (24), shown at the bottom of this page.

The above two parts can be calculated like (19) and (21). By the recursion, the probability $J_j = \mathbb{P}(w_{\pi_1} > \cdots > w_{\pi_{m+j}} > \beta_m \overline{w}_{m+1}^M > w_{\pi_{m+j+1}} > \cdots > w_{\pi_M})$ can be expressed as

$$J_j = \sum_{p=0}^{K-j} \mathbb{P}\Bigg(w_{\pi_1} > w_{\pi_2}, \cdots, w_{\pi_m} > w_{\pi_{m+1}}, \frac{\beta_m}{1-\beta_m} w_{\pi_{m+j}} - \sum_{\substack{i=m+2\\ i\neq m+j}}^{M} w_{\pi_i} > w_{\pi_{m+1}} > w_{\pi_{m+2}}, \cdots, w_{\pi_{m+j+p}} > \frac{\beta_m}{1-j\beta_m} \overline{w}_{m+j+1}^M > w_{\pi_{m+j+p+1}} > \cdots > w_{\pi_M} \Bigg) \quad (25)$$

where J_j contains $K - j + 1$ terms. Each term in J_j can be divided to the sum of a series probabilities based on the total probability except the first and the last one like (15). Consequently, the number of basic integration is $2^{K-j+1} - 1$. ■

When we make the assumption of $K > M - m$, the results will be different. Because of $K > M - m$, we can further have $\beta_m \overline{w}_{m+1}^M < \beta_m (M-m) w_{\pi_{m+1}} < w_{\pi_{m+1}}$. Then we draw the conclusion that the existing of the first probability like Q_1 contradicts with the assumption.

$$\Omega_{P^1_{J_{K-1}}} = \begin{cases} w_{\pi_{n+1}} < w_{\pi_n}, & n \in [1, m] \bigcup [m+K+1, M-1] \\ w_{\pi_{n+1}} < w_{\pi_n} < \frac{1}{n-m}\left(\frac{1-\beta_m}{\beta_m} w_{\pi_{m+K-1}} - \sum\limits_{\substack{i=n+1\\ i\neq m+K-1}}^{M} w_{\pi_i}\right), & n \in [m+1, m+K-2] \\ \frac{\beta_m}{1-(K-1)\beta_m} \overline{w}_{n+1}^M < w_{\pi_n}, & n = m+K-1 \\ w_{\pi_{n+1}} < w_{\pi_n} < \frac{\beta_m}{1-K\beta_m} \overline{w}_{n+1}^M, & n = m+K \\ 0 < w_{\pi_n}, & n = M \end{cases} \quad (23)$$

$$\Omega_{P^2_{J_{K-1}}} = \begin{cases} w_{\pi_{n+1}} < w_{\pi_n}, & n \in [1, m] \bigcup [m+K+1, M-1] \\ w_{\pi_{n+1}} < w_{\pi_n} < \frac{1}{n-m}\left(\frac{1-\beta_m}{\beta_m} w_{\pi_{m+K-1}} - \sum\limits_{\substack{i=n+1\\ i\neq m+K-1}}^{M} w_{\pi_i}\right), & n \in [m+1, m+K-2] \\ w_{\pi_{n+1}} < w_{\pi_n}, & n = m+K-1 \\ \frac{\beta_m}{1-k\beta_m} \overline{w}_{n+1}^M < w_{\pi_n}, & n = m+K \\ 0 < w_{\pi_n}, & n = M \end{cases} \quad (24)$$

For the last term of (14), the integration domain $\Omega_{P_{M-m}}$ for each variable is given by

$$\Omega_{P_{M-m}} = \begin{cases} w_{\pi_{n+1}} < w_{\pi_n}, & n \in [1, m] \\ w_{\pi_{n+1}} < w_{\pi_n} < \dfrac{1}{n-m}\left(\dfrac{1-\beta_m}{\beta_m} w_{\pi_M} - \sum_{i=n+1}^{M-1} w_{\pi_i}\right), & \\ \qquad n \in [m+1, M-2] & \\ w_{\pi_M} < w_{\pi_{M-1}} < \dfrac{1-(M-m-1)\beta_m}{\beta_m} w_{\pi_M}, & \\ \qquad n = M-1 & \\ 0 < w_{\pi_n}, & n = M \end{cases} \tag{26}$$

Since we make the assumption of $\beta_m < \frac{1}{M-m}$, $\frac{\beta_m}{1-(M-m-1)\beta_m} < 1$ always holds. Then the second last probability $\mathbb{P}\big(w_{\pi_1} > \cdots w_{\pi_{M-1}} > \beta_m \overline{w}_{m+1}^{M} > w_{\pi_M}\big)$only includes one probability, and the integration domain can be given by

$$\Omega_{P_{M-m-1}} = \begin{cases} w_{\pi_{n+1}} < w_{\pi_n}, & n \in [1, m] \\ w_{\pi_{n+1}} < w_{\pi_n} < \dfrac{1}{n-m}\left(\dfrac{1-\beta_m}{\beta_m} w_{\pi_{M-1}} - \sum_{i=n+1}^{M} w_{\pi_i}\right), & \\ \qquad n \in [m+1, M-2] & \\ w_{\pi_{n+1}} < w_{\pi_n}, & n = M-1 \\ 0 < w_{\pi_n}, & n = M \end{cases} \tag{27}$$

Similarly, the result of $\mathbb{P}(w_{\pi_m} > \overline{w}_{m+1}^{M}, \pi)$ could be derived by calculating 2^{M-m-1} probabilities based on the recursion method, and each probability can be calculated with the method similar to (26) and (27).

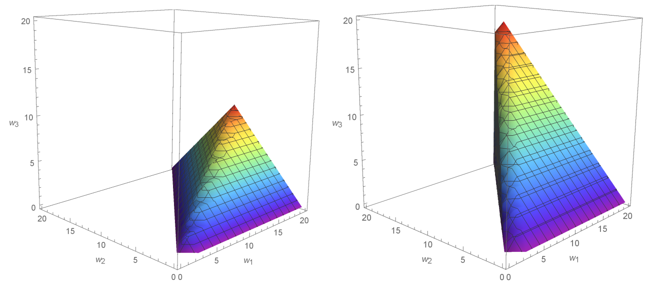

(a) (b)

FIGURE 1. The integral regions of three random variables w_1, w_2 and w_3 for user 1 when the decoding order is determined by $w_1 > w_2 > w_3$ of different target data rate of users for a 3-user NOMA system. The subfigure (a) illustrates the integral region of three random variables to obtain the outage probability of the user 1 when $\hat{R}_1 = \hat{R}_2 = \hat{R}_3 = 1$ and $\beta_1 = \beta_2 = \beta_3 = 1$; The subfigure (b) illustrates the integral region of three random variables when $\hat{R}_1 = \hat{R}_2 = \hat{R}_3 = 0.32$ and $\beta_1 = \beta_2 = \beta_3 = 0.25$.

To further illustrate the expression in (11), it is shown that the detailed integral regions of three random variables w_1, w_2 and w_3 to obtain the outage probability of the user 1 when the decoding order is determined by $w_1 > w_2 > w_3$ of different target data rate of users for a 3-user NOMA system in Fig.1. In Fig.1 (a), when $\beta_1 = \beta_2 = \beta_3 = 1$, the integral region is actually constrained by the decoding order and user's target data rate. While, in Fig.1 (b), the integral regions of three random variables is only constrained by the decoding order when $\beta_1 = \beta_2 = \beta_3 = 0.25$. In general, both of these cases could be obtained by the proposed method. Besides, when the number of serving users increases in the uplink NOMA system, the integral regions of (11) could also be elaborated based on the proposed method even though the higher dimensional integral diagram is not easy to display anymore.

Besides, for the last decoded user, the conditional probability $\mathbb{P}(E_{M|\pi}^{c})$ is given by

$$\begin{aligned} \mathbb{P}(E_{M|\pi}^{c}) &= \mathbb{P}(w_M > \beta_M \sigma^2, \pi) \\ &= \int_{\beta_M \sigma^2}^{\infty} \lambda_M e^{-\lambda_M w_M} \mathrm{d}w_M \cdots \int_{w_2}^{\infty} \lambda_1 e^{-\lambda_1 w_1} \mathrm{d}w_1 \\ &= \frac{\prod_{i=2}^{M} \lambda_{\pi_i} e^{-\sum_{i=1}^{M} \lambda_{\pi_i} \beta_M \sigma^2}}{\prod_{i=2}^{M} (\sum_{k=1}^{i} \lambda_{\pi_k})}. \end{aligned} \tag{28}$$

Above all, we can obtain the closed-form expression of the probability $E_{m|\pi}^{c}$ under the condition of the rate threshold β_m and the total number of accessing users M.

B. THEORETICAL ANALYSIS FOR FIXED-ORDERED SIC RECEIVER

In this section, the outage probability for the fixed ordered SIC receiver in the interference-limited uplink NOMA system is investigated. The decoding order is determined based on users' path loss. The achievable data rate R_m for the user m ($m \neq M$) is given by

$$R_m = \log\left(1 + \frac{w_m}{\sum_{i=m+1}^{M} w_i}\right). \tag{29}$$

And for the last decoded user M, the achievable data rate is expressed as

$$R_M = \log\left(1 + \frac{w_M}{\sigma^2}\right). \tag{30}$$

We define the event E_m^c that the m-th user's achievable data rate R_m is larger than its target data rate $\hat{R}_m$. Then we have

$$\mathbb{P}(E_m^c) = \begin{cases} \mathbb{P}\left(w_m \geq \alpha_m \sum_{i=m+1}^{M} w_i\right), & m \neq M \\ \mathbb{P}(w_m \geq \alpha_m \sigma^2), & m = M \end{cases} \tag{31}$$

where $\alpha_m = 2^{\hat{R}_m} - 1$.

Accordingly, we can derive the closed-form equation for the probability of the event E_m^c when $m \neq M$ with the fixed decoding order as following

$$\begin{aligned} &\mathbb{P}(w_m \geq \alpha_m \sum_{i=m+1}^{M} w_i) \\ &= \int_0^{\infty} \lambda_M e^{-\lambda_M w_M} \mathrm{d}w_M \cdots \int_{\beta_m(\sum\limits_{i=m+1}^{M} w_i + \frac{1}{\rho})}^{\infty} \lambda_m e^{-\lambda_m w_m} \mathrm{d}w_m \\ &= \frac{\prod\limits_{i=m+1}^{M} \lambda_i}{\prod\limits_{i=m+1}^{M} (\lambda_i + \alpha_m \lambda_m)}. \end{aligned} \tag{32}$$

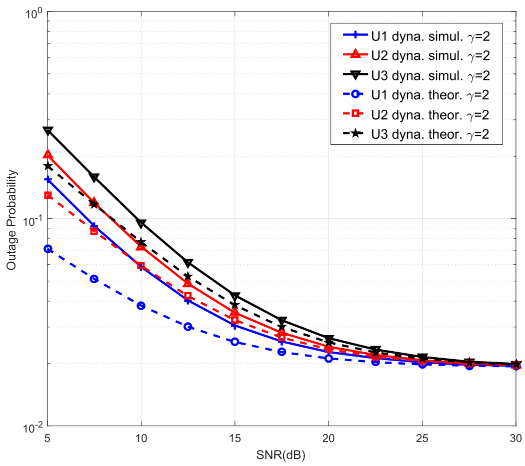

(a)

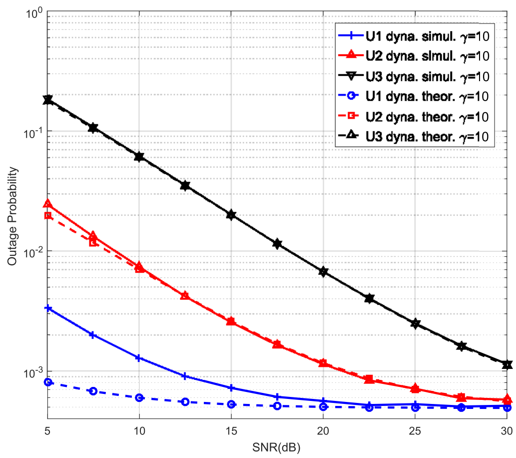

(b)

FIGURE 2. **The outage probability for the dynamic-ordered SIC receiver ((a)$\gamma = 2$ and (b) $\gamma = 10$) vs. SNR.**

The close-form expression of the last decoded user can be achieved by integral of the random variable w_M

$$\mathbb{P}(w_M \geq \alpha_M \sigma^2) = \int_{\alpha_M \sigma^2}^{\infty} \lambda_M e^{-\lambda_M w_M} \mathrm{d}w_M = e^{-\lambda_M \alpha_M \sigma^2}. \quad (33)$$

Finally, substituting (32) and (33) into (34), we can have the outage probability of the m-th user, which is given by

$$\mathbb{P}_m^{out} = 1 - \prod_{i=1}^{m} \mathbb{P}(E_i^c). \quad (34)$$

IV. NUMERICAL RESULTS

In this section, to achieve more insights of the analytical results, we provide the theoretical evaluations and the Monte Carlo simulations for a 3-user NOMA system. It is assumed that the path loss of each user can be offset by the path loss compensation part [9], [12]. To cancel the co-channel

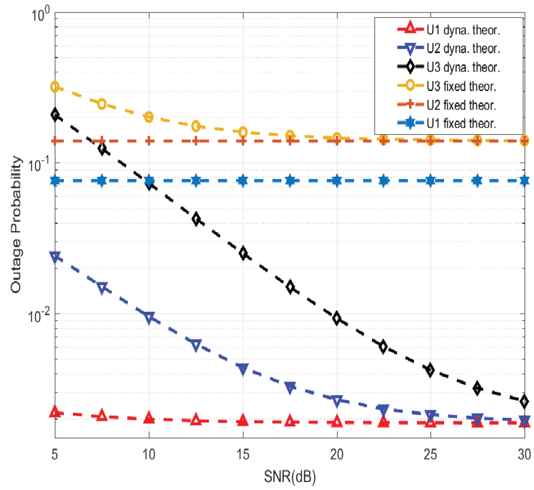

FIGURE 3. **The outage probability of three users vs. SNR for two types of receivers.**

interferences successively, we set a power back-off coefficient γ, which means that the transmit signal power of the user $(i-1)$ is γ dB stronger than that of the user i. Without loss of generality, the received signal to noise ratio is defined as $SNR = \frac{P}{\sigma^2}$, where P is set as the received power for the user with the worst large-scale fading.

In Fig.2, the outage probability of each user versus SNR is investigated for the dynamic ordered SIC. We set $\gamma = 2$ in Fig.2 (a) and $\gamma = 10$ in Fig.2 (b) to compare the influence of power back-off coefficients. For the two cases, the target rates for the three users are set equal to 0.7 bps/Hz. In low SNR region, it can be observed that there is a subtle gap between the theoretical results and simulation ones. This phenomenon should attribute to the fact that the additive Gaussian noise neglected in the theoretical results actually dominates the main interference in this case. Meanwhile, with the increase of SNR, the theoretical curves match better with the simulation ones, which corroborates the validity of the theoretical analysis. Besides, it is shown that the larger γ contributes to the lower outage probability of each user because the divergence in the power domain offers more advantage for the SIC receiver to distinguish the superimposed signals. And when the target data rate of each user is same, the larger γ make the interference from users more weaker which results in the great gaps of users.

The outage probabilities of the dynamic-ordered and fixed-ordered SIC receivers are presented in Fig.3. In this part, γ = 10dB and all the three users' target data rate are 0.8 bps/Hz. It can be observed that the dynamic ordered scheme outperforms the fixed one in terms of the outage probability. Moreover, the performance of the users is more balanced. The intuition behind this observation is that the dynamic strategy could guarantee the smallest multiuser interference for each user by adjusting the decoding order based on the instantaneous receiving power dynamically.

V. CONCLUSION

In this paper, we focus on the dynamic-ordered SIC receiver and the fixed-ordered one in the wireless uplink NOMA systems. The closed-form outage probability expressions are derived for each specific user under the i.ni.d. Rayleigh fading environment for both two types of SIC receivers, with the arbitrary number of the users. Furthermore, the accuracy of the theoretical expressions is verified by the Monte Carlo simulations. The numerical results show that the dynamic ordered scheme can achieve better outage performance than the fixed one. And the larger power back-off coefficient contributes to the lower outage probability for each user based on the dynamic scheme.

REFERENCES

[1] Z. Ding, X. Lei, G. K. Karagiannidis, R. Schober, J. Yuan, and V. K. Bhargava, "A survey on non-orthogonal multiple access for 5G networks: Research challenges and future trends," *IEEE J. Sel. Areas Commun.*, vol. 35, no. 10, pp. 2181–2195, Oct. 2017.

[2] Y. Yuan *et al.*, "Non-orthogonal transmission technology in LTE evolution," *IEEE Commun. Mag.*, vol. 54, no. 7, pp. 68–74, Jul. 2016.

[3] Y. Zhang, H. M. Wang, T. X. Zheng, and Q. Yang, "Energy-efficient transmission design in non-orthogonal multiple access," *IEEE Trans. Veh. Technol.*, vol. 66, no. 3, pp. 2852–2857, Mar. 2017.

[4] C. Yang, B. Xia, W. Xie, K. Huang, Y. Yao, and Y. Zhao, "Interference cancellation at receivers in cache-enabled wireless networks," *IEEE Trans. Veh. Technol.*, to be published, doi: 10.1109/TVT.2017.2739639.

[5] K. Xiao, B. Xia, Z. Chen, J. Wang, D. Chen, and S. Ma, "On optimizing multicarrier-low-density codebook for GMAC with finite alphabet inputs," *IEEE Commun. Lett.*, vol. 21, no. 8, pp. 1811–1814, Aug. 2017.

[6] H. Tabassum, E. Hossain, and J. Hossain, "Modeling and analysis of uplink non-orthogonal multiple access in large-scale cellular networks using Poisson cluster processes," *IEEE Trans. Commun.*, vol. 65, no. 8, pp. 3555–3570, Aug. 2017.

[7] Z. Ding *et al.*, "Impact of user pairing on 5G nonorthogonal multiple-access downlink transmissions," *IEEE Trans. Veh. Technol.*, vol. 65, no. 8, pp. 6010–6023, Aug. 2016.

[8] X. Yue, Y. Liu, S. Kang, and A. Nallanathan, "Performance analysis of NOMA with fixed gain relaying over Nakagami-*m* fading channels," *IEEE Access*, vol. 5, pp. 5445–5454, 2017.

[9] N. Zhang, J. Wang, G. Kang, and Y. Liu, "Uplink nonorthogonal multiple access in 5G systems," *IEEE Commun. Lett.*, vol. 20, no. 3, pp. 458–461, Mar. 2016.

[10] M. S. Ali, H. Tabassum, and E. Hossain, "Dynamic user clustering and power allocation for uplink and downlink non-orthogonal multiple access (NOMA) systems," *IEEE Access*, vol. 4, pp. 6325–6343, 2016.

[11] Z. Yang, Z. Ding, P. Fan, and N. Al-Dhahir, "A general power allocation scheme to guarantee quality of service in downlink and uplink NOMA systems," *IEEE Trans. Wireless Commun.*, vol. 15, no. 11, pp. 7244–7257, Nov. 2016.

[12] Y. Gao, B. Xia, K. Xiao, Z. Chen, X. Li, and S. Zhang, "Theoretical analysis of the dynamic decode ordering sic receiver for uplink NOMA systems," *IEEE Commun. Lett.*, vol. 21, no. 10, pp. 2246–2249, Oct. 2017.

[13] C. Li, B. Xia, S. Shao, Z. Chen, and Y. Tang, "Multi-user scheduling of the full-duplex enabled two-way relay systems," *IEEE Trans. Wireless Commun.*, vol. 16, no. 2, pp. 1094–1106, Feb. 2017.

[14] Z. Zhang, H. Sun, and R. Q. Hu, "Downlink and uplink non-orthogonal multiple access in a dense wireless network," *IEEE J. Sel. Areas Commun.*, vol. 35, no. 12, pp. 2771–2784, Dec. 2017.

[15] C. Li, Z. Chen, Y. Wang, Y. Yao, and B. Xia, "Outage analysis of the full-duplex decode-and-forward two-way relay system," *IEEE Trans. Veh. Technol.*, vol. 66, no. 5, pp. 4073–4086, May 2017.

[16] B. Xia, Y. Liu, C. Yang, Z. Chen, W. Xie, and Y. Zhao, "Opportunistic channel sharing in stochastic networks with dynamic traffic," *IEEE Trans. Veh. Technol.*, vol. 66, no. 10, pp. 9587–9591, Oct. 2017.

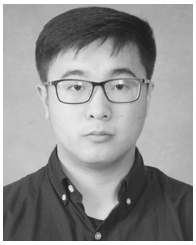

JINGLUN WANG received the B.Eng. degree from the School of Electronic Information and Electrical Engineering, Shanghai Jiao Tong University, Shanghai, China, in 2016, where he is currently pursuing the master's degree at the Department of Electronic Engineering, Institute of Wireless Communications Technology. His research expertise and interests include non-orthogonal multiple access in 5G mobile communication systems and wireless communication.

BIN XIA (M'11–SM'11) received the B.Eng. degree in electrical engineering and M.Eng. degree in information and communication engineering from the University of Science and Technology of China, Hefei, China, in 1997 and 2000, respectively, and the Ph.D. degree in electrical engineering from The University of Hong Kong, Hong Kong, in 2004. From 1995 to 2000, he was a Research Engineer with the Personal Communication and Spread Spectrum Laboratory, University of Science and Technology of China, involved with the development of CDMA communication systems based on IS-95 and UMTS standards. From 1999 to 2001, he was a Department Manager with UTStarcom Inc., involved with WCDMA systems. From 2004 to 2005, he was a System Engineer with Alcatel Shanghai Bell Co., Ltd., involved with UMTS and WiMAX systems. From 2005 to 2012, he was a Senior Research Scientist, a Project Manager, and the Director of Huawei Technologies Co., Ltd., involved with beyond 3G research and 4G LTE R&D. Since 2012, he has been a Professor with the Department of Electronic Engineering, Shanghai Jiao Tong University. His research interests are in the areas of coded modulation, MIMO, OFDM, crosslayer design, and radio network architecture.

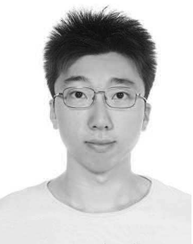

KEXIN XIAO received the B.Eng. degree from the School of Electronics and Information Engineering, Harbin Institute of Technology, Harbin, China, in 2014. He is currently pursuing the Ph.D. degree at the Department of Electronic Engineering, Institute of Wireless Communications Technology, Shanghai Jiao Tong University, Shanghai, China. His research expertise and interests include non-orthogonal multiple access and coded modulation in 5G mobile communication systems.

YICHEN GAO received the B.Eng. degree from the School of Electronic Information and Electrical Engineering, Shanghai Jiao Tong University (SJTU), Shanghai, China, in 2016, where he is currently pursuing the master's degree at the Department of Electronic Engineering, Institute of Wireless Communications Technology. His research expertise and interests include non-orthogonal multiple access in 5G mobile communication systems and wireless communication.

SHAODAN MA received the double bachelor's degrees in science and economics and master's degree in engineering from Nankai University, Tianjin, China, and the Ph.D. degree in electrical and electronic engineering from The University of Hong Kong, Hong Kong, in 2006. From 2006 to 2011, she was a Post-Doctoral Fellow with The University of Hong Kong. Since 2011, she has been with the University of Macau, where she is currently an Associate Professor. She was a Visiting Scholar with Princeton University, in 2010. She is currently an Honorary Assistant Professor with The University of Hong Kong. Her research interests are in the general areas of signal processing and communications, particularly, transceiver design, resource allocation, and performance analysis.